Advanced in vitro models for studying drug induced toxicity
Ramaiahgari, S.C.

Citation
Ramaiahgari, S. C. (2014, June 4). *Advanced in vitro models for studying drug induced toxicity*. Department of Toxicology, Leiden Academic Center for Drug Research (LACDR), Faculty of Science, Leiden University. Retrieved from https://hdl.handle.net/1887/25852

Cover Page

Universiteit Leiden

The handle http://hdl.handle.net/1887/25852 holds various files of this Leiden University dissertation

Author: Ramaiahgari, Sreenivasa Chakravarthy
Title: Advanced in vitro models for studying drug induced toxicity
Issue Date: 2014-06-04

CHAPTER 4

SYSTEMIC COMPARISON OF DICLOFENAC INDUCED GENE EXPRESSION CHANGES IN DIVERSE *IN VITRO* AND *IN VIVO* MODELS AND SPECIES

Sreenivasa C. Ramaiahgari[1], Steven Wink[1], Mackenzie Hadi[3],
John Meerman[1], Mirjam Luijten[2], Geny Groothuis[3],
Bob van de Water[1] and Leo S. Price[1]

[1]Division of Toxicology, Leiden Academic Centre for Drug Research,
Leiden University, Leiden, The Netherlands.

[2]Laboratory for Health Protection Research,
National Institute for Public Health and the Environment,
Bilthoven, The Netherlands.

[3]Division of Pharmacokinetics, Toxicology and Targeting,
Department of Pharmacy, University of Groningen,
Groningen, The Netherlands.

ABSTRACT

Drug-induced liver injury (DILI) is a major clinical concern. Various models are proposed to investigate DILI, but a gold-standard model that could predict human DILI is still lacking. A systematic comparison of *in vitro*/*in vivo* models would help to characterize the responses associated with the drug-induced hepatotoxicity and identify better model(s) that could closely predict human DILI. Here we performed a comparative transcriptomic analysis using ex-vivo human precision cut liver slices (PCLS), *in vitro* primary human hepatocytes, mouse hepatocytes, rat hepatocytes, the human hepatoma cell line HepG2, cultured in 2D monolayer or 3D spheroids, and *in vivo* rat and mouse livers. All models were exposed to the drug diclofenac, which causes idiosyncratic DILI. To dissect the canonical cellular stress responses upon diclofenac treatment in the different models we used Ingenuity pathway analysis, where human PCLS with its heterogeneous cell population representing intact liver tissue was used as a reference for all other models. Protein ubiquitination, Nrf2-associated oxidative stress and xenobiotic metabolism pathways were found to be significantly altered upon diclofenac treatment. Genes involved in liver diseases including cholestasis and steatosis were significantly upregulated providing an early evidence for long-term effects of diclofenac treatment. HepG2 cells in 3D culture were more responsive and showed a significant upregulation of stress signaling pathways and genes related to diclofenac induced liver diseases with a similarity to human PCLS. Compared to mouse, rat gene expression profiles were more similar to human gene expression. In conclusion, transcriptomic analysis will allow us to identify various drug-induced cellular stress responses. Functionally and phenotypically stable HepG2 spheroids could serve as a better alternative model to identify human relevant biomarkers of DILI.

INTRODUCTION

Adverse drug reactions are a major concern for the safe use of drugs. These reactions are undetected during early clinical trials in small groups of patients and are often idiosyncratic in nature [1]. With the first pass effect and its central role in drug metabolism, the liver is prone to adverse drug reactions leading to drug induced liver injury (DILI) or causing liver diseases after chronic treatment. DILI has been the major reason for pre- and post-marketed attrition of drugs [2]. There is an urgent need for improved methods and models that could reflect drug metabolism in a human system and ultimately predict DILI risk during early preclinical drug development.

Animal models are the primary source for toxicity studies, as they are the only available laboratory models with the complexity approaching that of humans. But several studies have shown that the toxicity assessment using animal models and its translation to human toxicological responses is quite poor [3]. In order to predict human DILI, human cell-based models possessing tissue specific characteristics are preferred. Current *in vitro* models are not feasible for long-term culture giving us no choice but to rely on animal models for studying repeated drug exposure effects. Ex-vivo models such as precision cut liver slices (PCLS) can represent an intact functional liver with heterogeneous cell population [4], which could respond similar to *in vivo* liver tissue [5]. But, major disadvantages of liver slices are a rapid decline of its functional properties ex vivo [6] and the low throughput limiting its value in repeated dose-effect studies. Primary human hepatocytes are considered as gold standards for compound screening assays [7]. But they also show a rapid decline of liver function and due to its high variability between donors; even replicate samples of a single transcriptomic study can differ [8]. In this respect, immortalized cell lines might provide an advantage in maintaining a stable gene expression and models using HepG2 and HepaRG have been studied for their efficiency in toxicogenomics [9, 10]. Recent developments in *in vitro* cell culture methodologies have helped to maintain the differentiated phenotype of cells for extended periods [11-14]. Systems such as bioreactors, micropatterning and ECM gels for 3D growth have been proposed that provide a physiological niche to various primary and immortal cell lines. Due to the ease of use and availability of HepG2 cells and the ability to maintain a highly differentiated spheroid phenotype with improved metabolic competence in 3D cultures [14], HepG2 spheroids could be an optimal choice for the evaluation of DILI. Drug-induced cytotoxicity is typically identified by simple cell death measurements in *in vitro* models. For accurate human translation it is important to determine whether the molecular initiation events and the subsequent cell state changes that trigger cytotoxicity are translatable from simple *in vitro* models to humans.

Genome-wide microarray analysis allows the detailed evaluation of altered gene expression upon toxic insults, thereby representing the altered cell status after drug-induced cellular perturbations. Likewise, such a transcriptomics analysis is highly suited to identify the cellular stress responses that underlie DILI-related cytotoxicity as well as the comparison of such stress responses between models. A wealth of toxicogenomics data from human, mouse, rat, canine *in vitro* and *in vivo* liver models has helped to identify promising biomarkers for liver injury [15]. These toxicogenomics data are available in the public domain Gene Expression Omnibus (GEO) [16], Array Express [17], Comparative Toxicogenomics Database (CTD) [18], EDGE [19, 20], Chemical Effects in Biological Systems (CEBS) [21], TG-GATES (Genomics Assisted Toxicity Evaluation System). TG-GATES has a database of *in vivo* and *in vitro* gene expression profiles of liver and kidney upon exposure to 150 chemicals, mainly drugs that are currently used for patients [22]. These databases can be used as a reference for comparing the gene expression profiles in different models upon exposure to toxicants relevant for DILI.

In the present study we compared the gene expression profiles of human PCLS, primary human hepatocytes, HepG2 cells, mouse primary hepatocytes, mouse liver, rat primary hepatocytes and rat liver treated with a widely used non-steroidal anti-inflammatory drug diclofenac. Diclofenac is one of the most frequent causes of adverse drug injury to the liver, with 180 confirmed cases reported by FDA during the initial marketing period [23]. Several possible mechanisms of diclofenac induced liver injury have been proposed which involve formation of reactive metabolites, mitochondrial injury, ROS formation as well as interference with the immune system signaling, but the molecular mechanism leading to the liver damage is largely unknown [24-26].

Using Ingenuity pathway analysis, molecular pathways that were altered upon diclofenac exposure in human PCLS, rat and mouse *in vivo*, human, rat and mouse cultured primary hepatocytes, and human hepatoma cell line HepG2 cultured in 2D monolayer or 3D spheroids were compared and a similarity of gene expression profiles at the pathway level was analyzed across species. Since fresh PCLS most closely represented *in vivo* human liver tissue, it was used as a standard reference for the other models. Genes associated with diclofenac-induced chronic liver injury were found to be significantly activated in human PCLS. Several xenobiotic metabolism and stress-induced pathways were significantly enriched highlighting their potential role in diclofenac induced liver injury. HepG2 spheroid cultures were more responsive than 2D HepG2 cultures and showed a high similarity to PCLS. Ingenuity classified toxicity-related pathways of HepG2 spheroids were very similar to PCLS.

MATERIALS AND METHODS

Cell culture and diclofenac exposure

HepG2 cells: HepG2 cell line was obtained from American type tissue culture (ATCC, Wesel, Germany), cultured in Dulbecco's modified Eagles medium (DMEM) supplemented with 10% (v/v) fetal bovine serum, (Invitrogen, The Netherlands), 25 U/mL penicillin and 25 µg/mL streptomycin (PSA, Invitrogen) and used for culture. 3D cultures were prepared as described earlier [14]. 500 µM Diclofenac (Sigma Aldrich, Zwijndrecht, The Netherlands) was incubated for 24 hours before RNA extraction. HepG2 cells in 2D culture were incubated with 500 µM diclofenac for 14 hours before RNA extraction. Human PCLS: Human PCLS were prepared and incubated with diclofenac as described earlier [27] Mouse liver and hepatocytes: Mouse hepatocytes were obtained as described earlier [28] and exposed with 500 µM diclofenac. Rat liver and hepatocytes: Rat liver and hepatocyte data was obtained from public transcriptomics data base, Toxicogenomics Project-Genomics Assisted Toxicity Evaluation system' (TG-GATEs). Rat *in vitro* hepatocytes were treated with 400 µM diclofenac for 24 h. Rat *in vivo* data single exposure with 100 mg/kg for 24 hours and for repeat exposures 100mg/kg daily dose via gavage until day 29 were used for analysis. Primary human hepatocytes: data set from primary human hepatocytes exposed with 400 µM diclofenac for 24 h obtained from public transcriptomics data base, Toxicogenomics Project-Genomics Assisted Toxicity Evaluation system' (TG-GATEs) was used for analysis.

RNA extraction for microarrays

Total RNA was extracted from 3D cultured HepG2 cells using Tri reagent (Sigma) followed by clean up using RNeasy® mini kit (Qiagen, Venlo, The Netherlands). Purity and concentration of the RNA were analyzed using NanoDrop ND-1000 spectrophotometer (Nanodrop technologies, Wilmington, DE, USA). RNA quality and integrity was further determined using the Agilent bioanalyser (Agilent Technologies Inc, Santa Clara, CA, USA). Biotinylated cRNA was prepared using the Affymetrix 3' IVT-Express Labeling Kit (Affymetrix, Santa clara, CA, USA) and hybridization steps were performed by Service XS B.V (Leiden, The Netherlands) on Affymetrix HT Human Genome U133 plus PM plate. Array plates were scanned using the Affymetrix GeneTitan scanner.

Microarray analysis

Probe annotation was performed using the hthgu133pluspmhsentrezg.db package version 17.1.0 and Probe mapping was performed with hthgu133pluspmhsentrezg-cdf file downloaded from NuGO (http://nmg-r.bioinformatics.nl/NuGO_R.html).

Probe-wise background correction, between-array (within same datasets) normalization and probe set summaries calculation was performed using the RMA function of the Affy package (Affy package, version 1.38.1) [29, 30]. The normalized data were statistically analyzed for differential gene expression using a linear model [31, 32] with coefficients for each experimental group using the Limma package (Limma package, version 1.22.0; [30]). A contrast analysis was applied to compare each exposure with the corresponding vehicle control. For hypothesis testing the moderated t-statistics by empirical Bayes moderation was used followed by an implementation of the multiple testing correction of Benjamini and Hochberg.

Array and normalization quality control was performed with the arrayQualityMetrics, a bioconductor package for quality assessment of microarray data [33]. All analysis was performed in the R statistical language environment (R development core team 2012).

Pathway analysis

Differentially expressed genes with P<0.05 (and FDR <0.05) were uploaded onto Ingenuity Pathway Analysis IPA® (Ingenuity® systems, Redwood, CA, USA). Genes that were </> 1.5 fold changed compared to vehicle control were selected for pathway enrichment analysis. Activation of canonical pathways is predicted by calculating p-value using right-tailed Fisher Exact Test from the DEG's and p-values less than 0.05 (-log=1.3) are said to be significantly activated. Heatmap and hierarchical clustering using Pearson correlation was performed using TM4: MultiExperiment Viewer program [34].

Sl.no	Test model	DEG's	(up"$^\wedge$") or (down"$^\vee$") regulated	Diclofenac Conc.	Exposure time
1	Human liver slices	3737	(1690$^\wedge$/2047$^\vee$)	500 µM	24 h
2	Primary human hepatocytes	4165	(2125$^\wedge$/2040$^\vee$)	400 µM	24 h
3	HepG2 cells 3D	3183	(1523$^\wedge$/1660$^\vee$)	500 µM	24 h
4	HepG2 cells 2D	4241	(2246$^\wedge$/1995$^\vee$)	500 µM	14 h
5	Primary mouse hepatocytes	4012	(2073$^\wedge$/1939$^\vee$)	500 µM	24 h
6	In vivo mouse liver	500	(192$^\wedge$/308$^\vee$)	100 mg/kg	24 h
7	Primary rat hepatocytes	3421	(1973$^\wedge$/1448$^\vee$)	400 µM	24 h
8	*In vivo* rat liver	2461	(1073$^\wedge$/1388$^\vee$)	100 mg/kg	24 h
9	*In vivo* rat liver repeat exposure	1141	(573$^\wedge$ /568$^\vee$)	100 mg/kg	29 days

Table 1: Differentially expressed genes after diclofenac treatment in various *in vitro* and *in vivo* models. Selection was based on genes that are significant P<0.05, FDR<0.05.

RESULTS

Diclofenac induced differential gene expression in human and rodent models

Differentially expressed genes (FDR & $P<0.05$) upon diclofenac treatment in various models are as shown in table 1. This included in almost all cases a 24-hour time point post exposure, except 2D HepG2 cultures (14-hour) and a chronic exposure in rat *in vivo* model (29-day); *In vivo* mouse and rat (repeated exposure) had the lowest number of DEGs of all models models (Fig 1A). Next, transcriptomic changes induced by diclofenac were compared across all models. 471 DEG's were found to have an overlap in the human models (Fig 1B). IPA analysis demonstrated that these genes are functionally associated with signaling pathways including remodeling of epithelial adherens junction, NRF2 mediated oxidative stress response and p53-signaling pathway. A complete list of pathways associated with these 471 genes is shown in
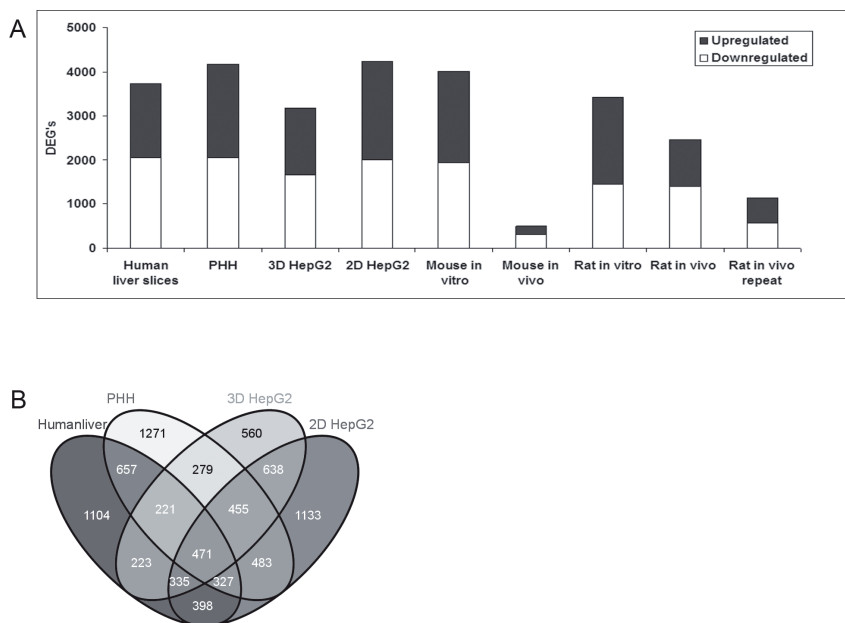

Figure 1: *Similarity of differentially expressed genes in various models*. Differentially expressed genes in various *in vitro*/*in vivo* models (A). Venn diagrams of DEG's from human derived cell lines (B); DEG's with $P<0.05$ (and FDR $P<0.05$) were selected.

supplementary figure S2. The overlap of DEGs in 2D/3D HepG2, hPCLS to primary hepatocyte models of human, mouse and rat was also analyzed: 214 genes were in common for 3D HepG2 spheroids; 242 for 2D HepG2 and 267 for human PCLS (Supplementary S2). Molecular pathways associated with these overlapping genes
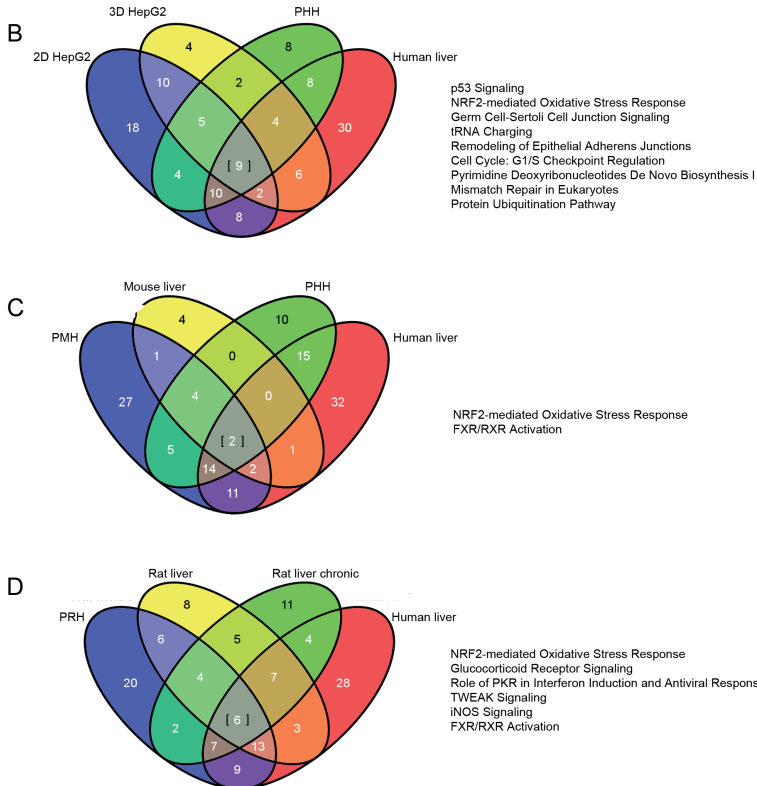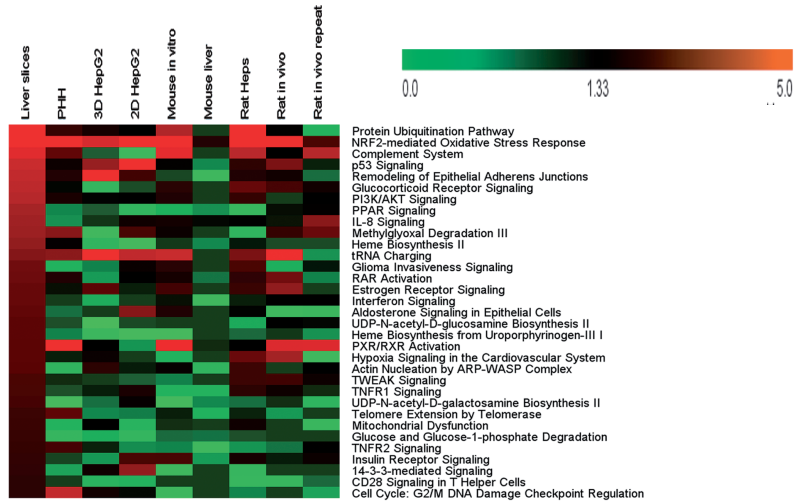
Figure 2: *Altered canonical pathways upon diclofenac exposure*. Heatmap showing significantly altered canonical pathways in human PCLS and their expression on other models from ingenuity pathway analysis (A). Venn diagram comparing significantly altered pathways in human cell models (B), Mouse models compared to human PCLS and PHH (C), Rat models compared to human PCLS (D). Significance calculated based on the ratio of the genes that are associated with specific canonical pathway, -log (p-value) 1.3 = P (0.05).

are as shown in supplementary S4. A closer similarity in overlapping pathways was seen between 3D HepG2 spheroids and human PCLS than 2D HepG2 and hPCLS (Supplementary S4). *In vivo* mouse liver exposed to diclofenac for 24 hours showed only 500 genes that were significantly changed, yet almost half of them overlapped with the mouse primary hepatocytes (Supplementary S1). Similarly, almost 50% of the DEGs of the single dose treatment of rat *in vivo* overlapped with the DEGs of the primary rat hepatocytes; also repeated diclofenac exposures in rats gave more than 60% concordance with either rat liver *in vivo* or rat hepatocytes *in vitro*. Venn diagrams showing association of DEG's between other models are in supplementary S1. Overall these data indicate that although there is quite a good concordance between all models, the highest concordance is reached within one species, either human, rat or mouse.

Differentially regulated canonical pathways upon diclofenac treatment
Although the overlap between the DEGs between species was relatively low, over-all, DEGs could be part of similar cellular stress response pathways. Therefore, for all the models the molecular pathways that are associated with DEG's from di-clofenac exposure were analyzed using Ingenuity Pathway Analysis (IPA®). We ranked the pathways of the different models according to the significance levels in the human PCLS model (Fig 2A). This demonstrates quite a differential mod-ulation of pathways in the different models. Significant activation of the Nrf2 ox-idative stress pathway was seen in all the models, highlighting its prime role in diclofenac induced liver injury. A higher number of significantly activated canoni-cal pathways are seen in mouse primary hepatocytes than mouse liver, which is due to less number of significant genes in mouse liver samples (Table 1).

Next we evaluated the overlap of the differentially modulated path-ways in the different models. Nine pathways had an overlap in human mod-els (Fig. 2B), which included some important stress pathways such as Nrf2 oxidative stress response and p53 signaling. Only two pathways overlapped between mouse models, PHH and human PCLS: Nrf2 pathway and PXR/RXR activation (Fig. 2A and C). Six pathways showed an overlap with rat mod-els and human PCLS, which also included Nrf2 signaling (Fig. 2A and D).

The pathways that are activated are not necessarily determined by the same gene sets. Therefore, for the most common pathways we first ex-tracted the genes that are significantly affected for the individual path-ways for the human PCLS model, and then extracted the fold change val-ues for all these individual genes from the other models. We focused on some of the top affected pathways that also contained sufficient DEGs (Fig. 3).
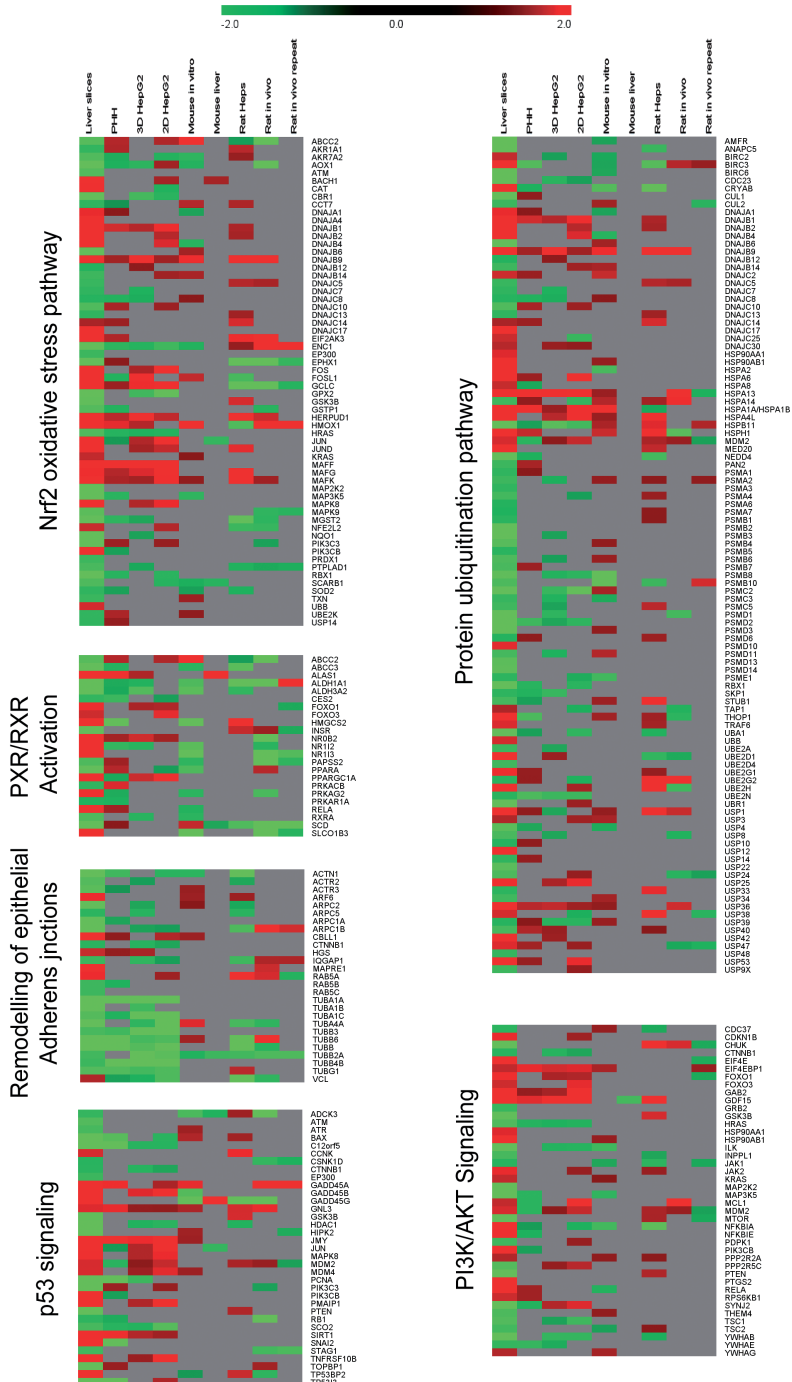
Figure 3: Individual genes associated with altered canonical pathways upon diclofenac treatment in human PCLS and their expression in other models. Fold change gene expression compared to vehicle controls.

Nrf2 oxidative stress response was a major common pathway that was induced upon diclofenac exposure. Diclofenac metabolites may cause mitochondrial impairment, ROS generation and subsequent oxidative stress, which is proposed as a possible mechanism of diclofenac-induced liver injury [35-38]. Oxidative stress activates the Nrf2 pathway to adapt to a more pro-oxidant environment. Genes regulated by Nrf2, such as HO-1 (heame oxygenase 1), are important markers for oxidative stress [39] and upregulation of HO-1 has been observed after diclofenac treatment [35, 36]. Here, HO-1 gene expression was seen in *in vivo* rodent models, human PCLS, primary hepatocytes and 3D HepG2 spheroids (Fig 3), but not in HepG2 cells in 2D culture in agreement with earlier reports [35]. This could be due to poor metabolism of diclofenac in 2D HepG2 cultures, since HO-1 expression was seen in HepG2 cells with S9 mixture [36]. In contrast, HepG2 cells cultured in hydrogels as spheroids expressed HO-1 supporting an increased metabolic competence in these HepG2 spheroids. Another Nrf2 target, DNAJB9, a HSP40 family protein, [40, 41] was induced >2-fold in human PCLS, rat primary cells and liver and 3D HepG2 cells. The expression of DNAJB9 was lower or not seen (mouse liver and rat repeated exposures) in other models (Fig 3). Interestingly, MafK expression was upregulated upon diclofenac exposure in all the models except mouse liver and rat chronic exposures where it was unchanged with diclofenac treatment (Fig 3). Nrf2/MafK heterodimer binds and activate anti-oxidant responsive elements (ARE), inducing the expression of phase II enzymes [42, 43]. It was also reported that over expression of MafK resulted in negative regulation of ARE-dependent transcription [44, 45]. The positive and negative regulation of antioxidant responsive elements by Nrf2/MafK may play an important role in balancing the oxidative stress response upon toxicant exposure.

Next we evaluated the p53 signaling pathway in more detail. Cellular injury-induced mitochondrial dysfunction and subsequent generation of ROS was shown to be involved in upstream activation of p53 mediated apoptotic signaling [46]. p53 plays a major role in DNA damage response, cell cycle regulation and apoptosis [47]. p53 signaling pathway is significantly altered upon diclofenac exposure in the all models studied, except mouse liver (Fig 2A). Downstream targets of p53 involved in cell cycle regulation and apoptosis showed a varied response in different models. GADD45a, is induced upon DNA damage and is involved in G2-M cell cycle arrest [48]. GADD45a is upregulated after diclofenac exposure in all the models except primary rat hepatocytes, 3D HepG2 and mouse liver (Fig 3A). Earlier studies have reported that diclofenac induces oxidative stress leading to DNA fragmentation and apoptotic cell death [49]. Activation of GADD45a may indicate induction of a DNA damage response upon diclofenac exposure in this study. Up regulation of p53 mediated apoptosis inducer, Bax, was seen only in mouse and rat primary hepatocytes (Fig 3A). MDM2, a negative regulator of p53 [50] was down-regulated in primary

human hepatocytes and rat repeated diclofenac exposures, but not differentially expressed in mouse models and is upregulated in other models.

PXR/RXR activation, PI3K/AKT signaling, protein ubiquitination pathway and remodeling of epithelial adherens junctions were all significantly altered upon diclofenac treatment. For these models the highest concordance for individual gene expression was observed amongst the human models. Overall these data indicate that, while in the different models diclofenac may activate similar pathways, overall the genes that are affected in these pathways is quite different. Most concordance is observed for species-specific changes. Regardless, some genes do overlap amongst all models, with the exception for mouse liver *in vivo* and rat repeated dose.
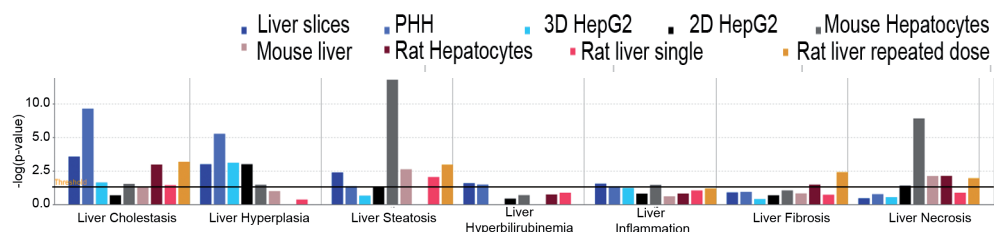

Figure 4. *Diclofenac induced gene expression changes associated with liver diseases*. Significance calculated based on the ratio of the genes that are associated with the onset or mechanism of liver disease manifestation, -log (p-value)1.3 = P 0.05 from Ingenuity Pathway Analysis.

Gene expression analysis identifies liver diseases associated with diclofenac treatment

Several cases have shown that long-term use of diclofenac lead to overt liver diseases. We used our transcriptomics data from different models to relate gene expression to disease models. FDA reports show that cholestasis was an adverse effect in 8% of patients taking diclofenac in 180 reported cases [23]. Analysis of genes involved in manifestation of liver diseases showed a significant induction of genes associated with cholestatic liver injury in all the models except 2D HepG2 cultures (Fig 4). Genes involved in liver hyperplasia were also significantly present in human cell models and mouse hepatocytes. Liver steatosis was significantly activated in human PCLS, primary human hepatocytes, 2D HepG2 cells, mouse and *in vivo* rat models. In particular, mouse primary hepatocytes showed a significant activation of genes involved in steatotic injury, ~4 fold higher than the human PCLS. Steatosis is not reported with diclofenac treatment in clinical use. Genes associated with liver hyperbilirubinemia and inflammation were significantly induced in human PCLS and primary human hepatocytes. Clinical cases associated with inflammation leading to hepatitis and hyperbilirubinemia were reported earlier with diclofenac use [51, 52]. Our data suggest that transcriptomic analysis could provide early evidence to potential drug-induced liver diseases.
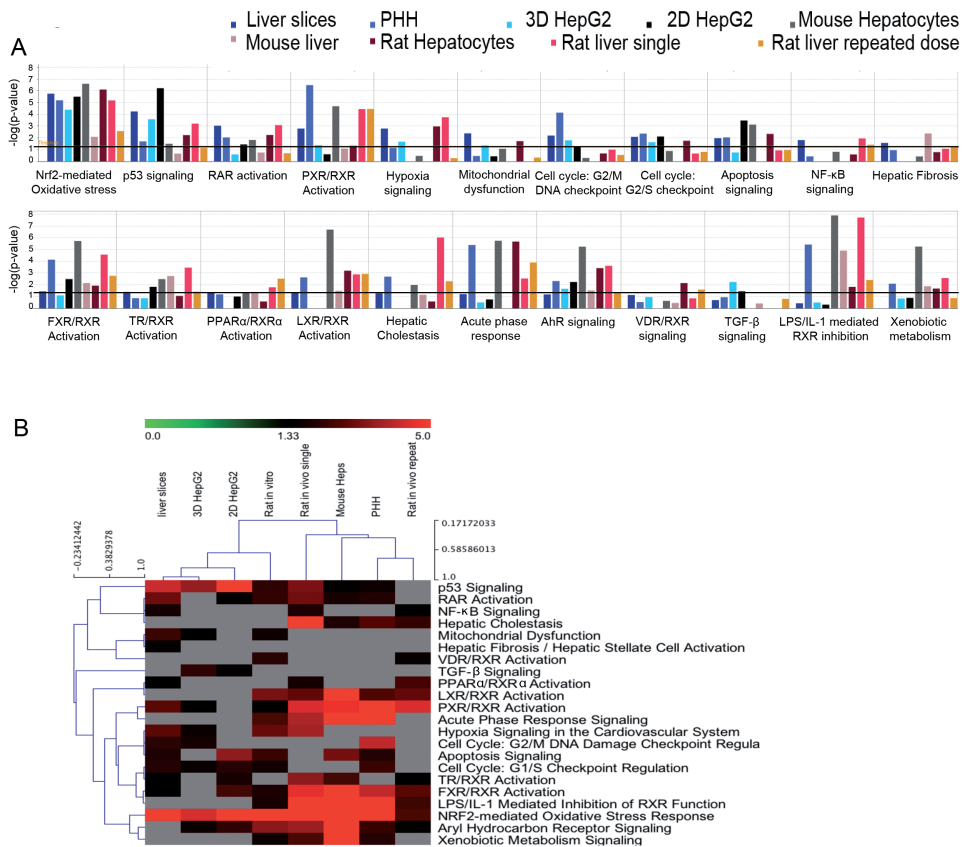
Figure 5. *Toxicity pathways from 'IPA Tox pathways' and their induction upon diclofenac treatment*. Canonical toxicity pathways in various models (A); Hierarchical clustering of toxicity pathways (B).

Toxicity pathways activated upon diclofenac exposure

Our initial IPA analysis involved all signaling pathways and networks, without a focus on pathways involved in toxicity. Therefore, as a final step we focused solely on pathways that are related to toxicity. 22 pathways that are listed in the IPA program that have a significant role in xenobiotic toxicity response were further analyzed (Fig. 5A and B). Overall, mouse hepatocytes and rat *in vivo* single dose showed the strongest toxicity pathway activation. Genes involved in mitochondrial dysfunction were significantly activated in human PCLS, 3D HepG2 spheroids and rat primary hepatocytes. Cell cycle pathways; G2/M and G2/S checkpoint were significantly activated in all human cell models and rat hepatocytes (Fig. 5A). NF-κB signaling was significantly active in human PCLS and *in vivo* rat models. Other xenobiotic metabolism pathways FXR/RXR, TR/RXR, LXR/RXR were primarily activated in rodent models. Pathways involved in inflammatory signaling and acute phase response signaling were significantly activated in primary human hepatocytes, mouse hepatocytes and

rat models (Fig 5A).

Next we performed unsupervised hierarchical clustering of toxicity pathways to determine which model was closest to human PCLS (Fig 5B). The 3D HepG2 spheroid model was in closest proximity to PCLS with high similarity in the activation of mitochondrial dysfunction, PXR/RXR pathway, p53 signaling, hypoxia signaling, cell cycle: G2/M DNA damage checkpoint regulation and Nrf2 signaling. All primary hepatocyte models were also in close similarity in particular with respect to PXR/RXR activation, AhR signaling, LXR/RXR activation, hepatic cholestasis.

DISCUSSION

With several *in vitro* and *in vivo* models in practical use as surrogates to study human specific DILI, comparative gene expression profiling of these models will provide an improved insight into the molecular changes that occur upon xenobiotic exposure. This type of comparative analysis will also help in characterizing the value of different *in vitro*/ *in vivo* models in predicting human specific responses associated with xenobiotic insult. In this study we used transcriptomics data to compare the effect of diclofenac treatment in human and rodent *in vitro*/*in vivo* models. Human PCLS showed a clear upregulation of molecular pathways that are associated with the pathogenicity of diclofenac induced liver injury. We anticipated a similar xenobiotic response in primary human hepatocytes (PHH). Although we observed a similar level of gene expression changes in PCLS and PHH, there were quite significant differences in the expression profile and even less similarities in the significantly affected cellular stress signaling pathways. Intriguingly, HepG2 cells cultured as spheroids showed diclofenac-induced activation of various stress signaling pathways comparable to human PCLS models; this was not observed in HepG2 cells cultured as 2D monolayer cells. This is likely due to increased metabolic competence observed in differentiated HepG2 spheroid cultures [14]. Phase 1 metabolism enzymes CYP2C9, CYP3A4 and phase II UGT's are involved in metabolism of diclofenac [37]; acyl glucuronides from glucuronosyl-transferse UGT2B7 and 4-hydroxy diclofenac from CYP2C9 are the major metabolites in diclofenac metabolism [53, 54]. These metabolites were previously shown to form in HepG2 spheroids exposed to diclofenac [14], suggesting a mechanistic response in HepG2 spheroids which is not seen in HepG2 2D cultures where drug metabolism enzymes are poorly expressed [55].

Diclofenac induces apoptosis by disrupting mitochondrial function and generating reactive oxygen species [24]. Genes that lead to mitochondrial dysfunction were seen only in human PCLS, 3D HepG2 spheroids and rat hepatocytes. Due to large inter-individual variability, primary human hepatocytes from 10 different cryopreserved donors were used for this transcriptomic study. However, the genes as-

sociated with mitochondrial dysfunction were not significantly activated in PHH, or in other primary hepatocytes or HepG2 cells in 2D culture. The differentiated HepG2 spheroids responded similarly to PCLS and rats treated with diclofenac, suggesting an increased functional complexity that has developed during differentiation of cells in 3D culture. Mitochondrial dysfunction has been proposed to be one of the underlying causes of idiosyncrasy [56, 57]; failure to identify mitochondrial toxicity in some models is a caveat for predictive toxicogenomics assays.

Nrf2-mediated oxidative stress response is a major signaling pathway that was reported in diclofenac hepatotoxicity and significantly activated in all the models in the current study. Earlier studies have shown that Heameoxyenase-1 (HO-1) in Nrf2 pathway is significantly induced upon diclofenac treatment [35]. Induction of HO-1 is seen in 3D HepG2 spheroids and other models compared in this study but not in 2D cultured HepG2 cells. FXR/RXR activation pathway was significantly activated upon diclofenac treatment in human (except 3D HepG2), rat and mouse models. FXR/RXR plays a role in bile acid regulation, lipid and glucose metabolism, [58] activation of drug metabolism enzymes [59] and protection against xenobiotic injury [60]. Activation of FXR/RXR pathway was also seen in diclofenac exposed rat livers in earlier studies [61] suggesting a role in diclofenac metabolism.

Genes and molecular events associated with diclofenac injury were highly enriched in DEG's from PCLS. PCLS may be a better alternative in understanding the short-term responses induced by the drugs, but its dependency on availability of human liver samples, variability due to different genetic backgrounds of individual samples and rapid decline of its native liver physiology have to be addressed for its relevance in exploring long-term effects of the xenobiotics. Similarly PHH have several limitations as described earlier for its dependence in toxicological assays. Although important stress signaling pathways such as Nrf2 oxidative stress pathway, genes associated with liver diseases such as cholestasis and steatosis were activated in both PCLS and PHH there was a considerable difference in activated pathways between PCLS and PHH.

DEG's in rat and mouse primary hepatocytes shared higher similarity to their *in vivo* counterparts than to human models. Mouse hepatocytes had similar enriched pathways as mouse *in vivo*, and in some aspects genes associated with liver diseases were significantly higher in mouse hepatocytes, although this may be due to the low number of DEG's in mouse *in vivo* treatments. DEG's in rat had higher similarity to humans than mouse, highlighting the increased capacity of rat compared to mouse in predicting human specific responses. Nonetheless, animal models are poor in predicting human responses and their current dependency is mainly due to lack of complex models that closely reflect complex human systems. Human derived immortalized hepatocytes with improved metabolic competence and polarized he-

patocyte morphology such as 3D HepG2 spheroids used in this study gave similar responses as PCLS. 3D HepG2 spheroids showed upregulation of genes and pathways that are associated with the mechanism of diclofenac injury, which were not seen in same cells cultured in a 2D monolayer. The ability to sustain a stable phenotype for a longer period whilst maintaining their polarized morphology and increased metabolic competence is also ideal for studying repeated dose effects of drugs.

In the current investigation we have used transcriptomics data from in-house and publicly available sources. Moreover, the isolation procedures and culturing protocols have been different for all individual models. In addition, concentrations of diclofenac, mRNA isolation and Affymetrix hybridization procedures may have been slightly different. Despite these discrepancies we find quite strong overlap in various pathways that are activated in the different models. Moreover, several individual genes that are modulated across different models and that represent individual pathway activation are likely ideal markers for cross species comparison and human translation. Future next generation sequencing approaches of similar comparative treatment samples across species and models will further limit the variability and likely identify additional candidate translational biomarkers for DILI.

In conclusion, this study provides an overview of transcriptional responses in various models upon diclofenac exposure and their commonality. The ability to predict long-term effects of diclofenac and its toxicity pathways at gene level further supports toxicogenomic approaches in predicting toxicity of new chemical entities. New improved *in vitro* models such as the HepG2 spheroid model used in this analysis would be valuable to consider in future toxicogenomic approaches.

REFERENCES

1   Naranjo, C. A., Busto, U. & Sellers, E. M. Difficulties in assessing adverse drug reactions in clinical trials. Progress in neuro-psychopharmacology & biological psychiatry 6, 651-657 (1982).

2   Kaplowitz, N. Idiosyncratic drug hepatotoxicity. Nat Rev Drug Discov 4, 489-499, doi:10.1038/nrd1750 (2005).

3   Knight, A. Systematic reviews of animal experiments demonstrate poor human clinical and toxicological utility. Altern Lab Anim 35, 641-659 (2007).

4   Graaf, I. A., Groothuis, G. M. & Olinga, P. Precision-cut tissue slices as a tool to predict metabolism of novel drugs. Expert opinion on drug metabolism & toxicology 3, 879-898, doi:10.1517/17425255.3.6.879 (2007).

5   Elferink, M. G. et al. Microarray analysis in rat liver slices correctly predicts in vivo hepatotoxicity. Toxicol Appl Pharmacol 229, 300-309, doi:10.1016/j.taap.2008.01.037 (2008).

6   de Graaf, I. A. et al. Preparation and incubation of precision-cut liver and intestinal slices for application in drug metabolism and toxicity studies. Nat Protoc 5, 1540-1551, doi:10.1038/nprot.2010.111 (2010).

7   LeCluyse, E. et al. Expression and regulation of cytochrome P450 enzymes in primary cultures of human hepatocytes. Journal of biochemical and molecular toxicology 14, 177-188 (2000).

8   Hart, S. N. et al. A comparison of whole genome gene expression profiles of HepaRG cells and HepG2 cells to primary human hepatocytes and human liver tissues. Drug metabolism and disposition: the biological fate of chemicals 38, 988-994, doi:10.1124/dmd.109.031831 (2010).

9   Jennen, D. G. et al. Comparison of HepG2 and HepaRG by whole-genome gene expression analysis for the purpose of chemical hazard identification. Toxicol Sci 115, 66-79, doi:10.1093/toxsci/kfq026 (2010).

10   Jetten, M. J., Kleinjans, J. C., Claessen, S. M., Chesne, C. & van Delft, J. H. Baseline and genotoxic compound induced gene expression profiles in HepG2 and HepaRG compared to primary human hepatocytes. Toxicol In Vitro 27, 2031-2040, doi:10.1016/j.tiv.2013.07.010 (2013).

11   Khetani, S. R. et al. Use of micropatterned cocultures to detect compounds that cause drug-induced liver injury in humans. Toxicol Sci 132, 107-117, doi:10.1093/toxsci/kfs326 (2013).

12   Guillouzo, A. et al. The human hepatoma HepaRG cells: a highly differentiated model for studies of liver metabolism and toxicity of xenobiotics. Chemico-biological interactions 168, 66-73, doi:10.1016/j.cbi.2006.12.003 (2007).

13   Gunness, P. et al. 3D organotypic cultures of human HepaRG cells: a tool for in vitro toxicity studies. Toxicol Sci 133, 67-78, doi:10.1093/toxsci/kft021 (2013).

14   Ramaiahgari et al. A 3D in vitro model of differentiated HepG2 cell spheroids with improved liver-like properties for repeated dose high-throughput toxicity studies. Archives of toxicology (2014).

15   Kiyosawa, N., Ando, Y., Manabe, S. & Yamoto, T. Toxicogenomic biomarkers for liver toxicity. Journal of toxicologic pathology 22, 35-52, doi:10.1293/tox.22.35 (2009).

16   Edgar, R., Domrachev, M. & Lash, A. E. Gene Expression Omnibus: NCBI gene expression and hybridization array data repository. Nucleic Acids Res 30, 207-210 (2002).

17   Brazma, A. et al. ArrayExpress--a public repository for microarray gene expression data at the EBI. Nucleic Acids Res 31, 68-71 (2003).

18   Mattingly, C. J., Rosenstein, M. C., Colby, G. T., Forrest, J. N., Jr. & Boyer, J. L. The Comparative Toxicogenomics Database (CTD): a resource for comparative toxicological studies. Journal of experimental zoology. Part A, Comparative experimental biology 305, 689-692, doi:10.1002/jez.a.307 (2006).

19   Hayes, K. R. et al. EDGE: a centralized resource for the comparison, analysis, and distribution of toxicogenomic information. Molecular pharmacology 67, 1360-1368, doi:10.1124/mol.104.009175 (2005).

20   Kiyosawa, N., Manabe, S., Yamoto, T. & Sanbuissho, A. Practical application of toxicogenomics for profiling toxicant-induced biological perturbations. International journal of molecular sciences 11, 3397-3412, doi:10.3390/ijms11093397 (2010).

21   Waters, M. et al. CEBS--Chemical Effects in Biological Systems: a public data repository integrating study design and toxicity data with microarray and proteomics data. Nucleic Acids Res 36, D892-900, doi:10.1093/nar/gkm755 (2008).

22   Uehara, T. et al. The Japanese toxicogenomics project: application of toxicogenomics. Molecu-

lar nutrition & food research 54, 218-227, doi:10.1002/mnfr.200900169 (2010).

23   Banks, A. T., Zimmerman, H. J., Ishak, K. G. & Harter, J. G. Diclofenac-associated hepatotoxicity: analysis of 180 cases reported to the Food and Drug Administration as adverse reactions. Hepatology 22, 820-827 (1995).

24   Gomez-Lechon, M. J. et al. Diclofenac induces apoptosis in hepatocytes by alteration of mitochondrial function and generation of ROS. Biochemical pharmacology 66, 2155-2167 (2003).

25   Bort, R., Ponsoda, X., Jover, R., Gomez-Lechon, M. J. & Castell, J. V. Diclofenac toxicity to hepatocytes: a role for drug metabolism in cell toxicity. J Pharmacol Exp Ther 288, 65-72 (1999).

26   Chung, H. et al. Comprehensive analysis of differential gene expression profiles on diclofenac-induced acute mouse liver injury and recovery. Toxicol Lett 166, 77-87, doi:10.1016/j.toxlet.2006.05.016 (2006).

27   Hadi, M. et al. Human precision-cut liver slices as an ex vivo model to study idiosyncratic drug-induced liver injury. Chemical research in toxicology 26, 710-720, doi:10.1021/tx300519p (2013).

28   Schaap, M. M. et al. Dissecting modes of action of non-genotoxic carcinogens in primary mouse hepatocytes. Arch Toxicol 86, 1717-1727, doi:10.1007/s00204-012-0883-6 (2012).

29   Irizarry, R. A. et al. Summaries of Affymetrix GeneChip probe level data. Nucleic Acids Res 31, e15 (2003).

30   Irizarry, R. A. et al. Exploration, normalization, and summaries of high density oligonucleotide array probe level data. Biostatistics 4, 249-264, doi:10.1093/biostatistics/4.2.249 (2003).

31   Smyth, G. K., Yang, Y. H. & Speed, T. Statistical issues in cDNA microarray data analysis. Methods Mol Biol 224, 111-136, doi:10.1385/1-59259-364-X:111 (2003).

32   Wolfinger, R. D. et al. Assessing gene significance from cDNA microarray expression data via mixed models. Journal of computational biology : a journal of computational molecular cell biology 8, 625-637, doi:10.1089/106652701753307520 (2001).

33   Kauffmann, A., Gentleman, R. & Huber, W. arrayQualityMetrics--a bioconductor package for quality assessment of microarray data. Bioinformatics 25, 415-416, doi:10.1093/bioinformatics/btn647 (2009).

34   Saeed, A. I. et al. TM4: a free, open-source system for microarray data management and analysis. BioTechniques 34, 374-378 (2003).

35   Cantoni, L. et al. Induction of hepatic heme oxygenase-1 by diclofenac in rodents: role of oxidative stress and cytochrome P-450 activity. Journal of hepatology 38, 776-783 (2003).

36   Miyamoto, Y., Ohshida, K. & Sasago, K. Protein assay for heme oxygenase-1 (HO-1) induced by chemicals in HepG2 cells. J Toxicol Sci 34, 709-714 (2009).

37   Tang, W. The metabolism of diclofenac--enzymology and toxicology perspectives. Current drug metabolism 4, 319-329 (2003).

38   Cosgrove, B. D. et al. Synergistic drug-cytokine induction of hepatocellular death as an in vitro approach for the study of inflammation-associated idiosyncratic drug hepatotoxicity. Toxicol Appl Pharmacol 237, 317-330, doi:10.1016/j.taap.2009.04.002 (2009).

39   Gu, Q. et al. Heme oxygenase-1 alleviates mouse hepatic failure through suppression of adaptive immune responses. J Pharmacol Exp Ther 340, 2-10, doi:10.1124/jpet.111.186551 (2012).

40   Fink, A. L. Chaperone-mediated protein folding. Physiol Rev 79, 425-449 (1999).

41   Thimmulappa, R. K. et al. Identification of Nrf2-regulated genes induced by the chemopreventive agent sulforaphane by oligonucleotide microarray. Cancer Res 62, 5196-5203 (2002).

42   van Bladeren, P. J. Glutathione conjugation as a bioactivation reaction. Chemico-biological interactions 129, 61-76 (2000).

43   Itoh, K. et al. An Nrf2/small Maf heterodimer mediates the induction of phase II detoxifying enzyme genes through antioxidant response elements. Biochemical and biophysical research communications 236, 313-322 (1997).

44   Nguyen, T., Huang, H. C. & Pickett, C. B. Transcriptional regulation of the antioxidant response element. Activation by Nrf2 and repression by MafK. J Biol Chem 275, 15466-15473, doi:10.1074/jbc.M000361200 (2000).

45   Dhakshinamoorthy, S. & Jaiswal, A. K. Small maf (MafG and MafK) proteins negatively regulate antioxidant response element-mediated expression and antioxidant induction of the NAD(P)H:Quinone oxidoreductase1 gene. J Biol Chem 275, 40134-40141, doi:10.1074/jbc.M003531200 (2000).

46   Karawajew, L., Rhein, P., Czerwony, G. & Ludwig, W. D. Stress-induced activation of the p53

tumor suppressor in leukemia cells and normal lymphocytes requires mitochondrial activity and reactive oxygen species. Blood 105, 4767-4775, doi:10.1182/blood-2004-09-3428 (2005).

47   Levine, A. J. p53, the cellular gatekeeper for growth and division. Cell 88, 323-331 (1997).

48   Jin, S. et al. GADD45-induced cell cycle G2-M arrest associates with altered subcellular distribution of cyclin B1 and is independent of p38 kinase activity. Oncogene 21, 8696-8704, doi:10.1038/sj.onc.1206034 (2002).

49   Hickey, E. J., Raje, R. R., Reid, V. E., Gross, S. M. & Ray, S. D. Diclofenac induced in vivo nephrotoxicity may involve oxidative stress-mediated massive genomic DNA fragmentation and apoptotic cell death. Free radical biology & medicine 31, 139-152 (2001).

50   Wang, X. p53 regulation: teamwork between RING domains of Mdm2 and MdmX. Cell Cycle 10, 4225-4229, doi:10.4161/cc.10.24.18662 (2011).

51   Sallie, R. W., McKenzie, T., Reed, W. D., Quinlan, M. F. & Shilkin, K. B. Diclofenac hepatitis. Australian and New Zealand journal of medicine 21, 251-255 (1991).

52   Ramakrishna, B. & Viswanath, N. Diclofenac-induced hepatitis: case report and literature review. Liver 14, 83-84 (1994).

53   King, C., Tang, W., Ngui, J., Tephly, T. & Braun, M. Characterization of rat and human UDP-glucuronosyltransferases responsible for the in vitro glucuronidation of diclofenac. Toxicol Sci 61, 49-53 (2001).

54   Leemann, T., Transon, C. & Dayer, P. Cytochrome P450TB (CYP2C): a major monooxygenase catalyzing diclofenac 4'-hydroxylation in human liver. Life sciences 52, 29-34 (1993).

55   Westerink, W. M. a. & Schoonen, W. G. E. J. Cytochrome P450 enzyme levels in HepG2 cells and cryopreserved primary human hepatocytes and their induction in HepG2 cells. Toxicology in vitro : an international journal published in association with BIBRA 21, 1581-1591, doi:10.1016/j.tiv.2007.05.014 (2007).

56   Liguori, M. J. et al. Microarray analysis in human hepatocytes suggests a mechanism for hepatotoxicity induced by trovafloxacin. Hepatology 41, 177-186, doi:10.1002/hep.20514 (2005).

57   Li, A. P. A review of the common properties of drugs with idiosyncratic hepatotoxicity and the "multiple determinant hypothesis" for the manifestation of idiosyncratic drug toxicity. Chemico-biological interactions 142, 7-23 (2002).

58   Matsukuma, K. E. et al. Coordinated control of bile acids and lipogenesis through FXR-dependent regulation of fatty acid synthase. Journal of lipid research 47, 2754-2761, doi:10.1194/jlr.M600342-JLR200 (2006).

59   Gnerre, C., Blattler, S., Kaufmann, M. R., Looser, R. & Meyer, U. A. Regulation of CYP3A4 by the bile acid receptor FXR: evidence for functional binding sites in the CYP3A4 gene. Pharmacogenetics 14, 635-645 (2004).

60   Lee, F. Y. et al. Activation of the farnesoid X receptor provides protection against acetaminophen-induced hepatic toxicity. Mol Endocrinol 24, 1626-1636, doi:10.1210/me.2010-0117 (2010).

61   Deng, X. et al. Gene expression profiles in livers from diclofenac-treated rats reveal intestinal bacteria-dependent and -independent pathways associated with liver injury. J Pharmacol Exp Ther 327, 634-644, doi:10.1124/jpet.108.140335 (2008).
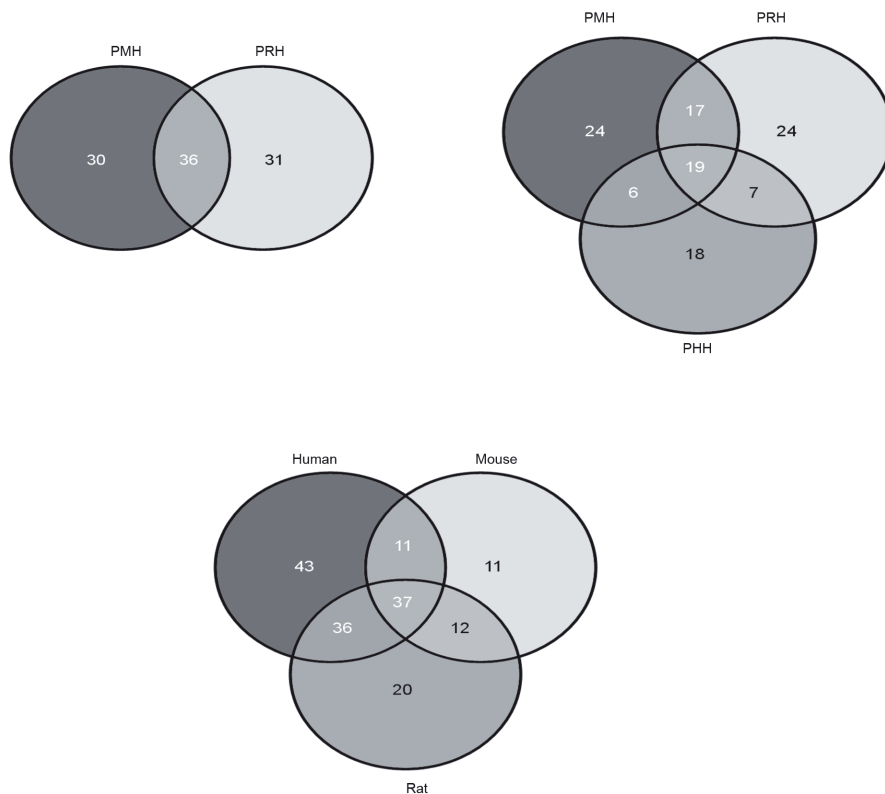
SUPPLEMENTARY DATA

Ingenuity Canonical Pathways	-log(p-value)
Remodeling of Epithelial Adherens Junctions	3.66E+00
tRNA Charging	2.63E+00
14-3-3-mediated Signaling	2.61E+00
Epithelial Adherens Junction Signaling	2.49E+00
NRF2-mediated Oxidative Stress Response	2.32E+00
Bladder Cancer Signaling	2.26E+00
p53 Signaling	1.95E+00
Sertoli Cell-Sertoli Cell Junction Signaling	1.94E+00
Gap Junction Signaling	1.88E+00
Germ Cell-Sertoli Cell Junction Signaling	1.83E+00
Activation of IRF by Cytosolic Pattern Recognition Receptors	1.78E+00
TCA Cycle II (Eukaryotic)	1.78E+00
Cell Cycle: G1/S Checkpoint Regulation	1.70E+00
Neuregulin Signaling	1.70E+00
Breast Cancer Regulation by Stathmin1	1.69E+00
IL-17A Signaling in Gastric Cells	1.63E+00
Thio-molybdenum Cofactor Biosynthesis	1.60E+00
Glutamate Removal from Folates	1.60E+00
Lipoate Salvage and Modification	1.60E+00
L-cysteine Degradation II	1.60E+00
Asparagine Biosynthesis I	1.60E+00
Chronic Myeloid Leukemia Signaling	1.57E+00
HMGB1 Signaling	1.55E+00
Guanosine Nucleotides Degradation III	1.46E+00
Prolactin Signaling	1.46E+00
Assembly of RNA Polymerase III Complex	1.40E+00
Role of IL-17A in Psoriasis	1.40E+00
Urate Biosynthesis/Inosine 5'-phosphate Degradation	1.40E+00
PDGF Signaling	1.37E+00
Thrombopoietin Signaling	1.32E+00
Lipoate Biosynthesis and Incorporation II	1.31E+00
Sulfate Activation for Sulfonation	1.31E+00
Cysteine Biosynthesis/Homocysteine Degradation	1.31E+00

Supplementary S1. Molecular Pathways associated with 471 overlapping genes in human cell models (from Figure 1B); as calculated by Ingenuity Pathway Analysis.
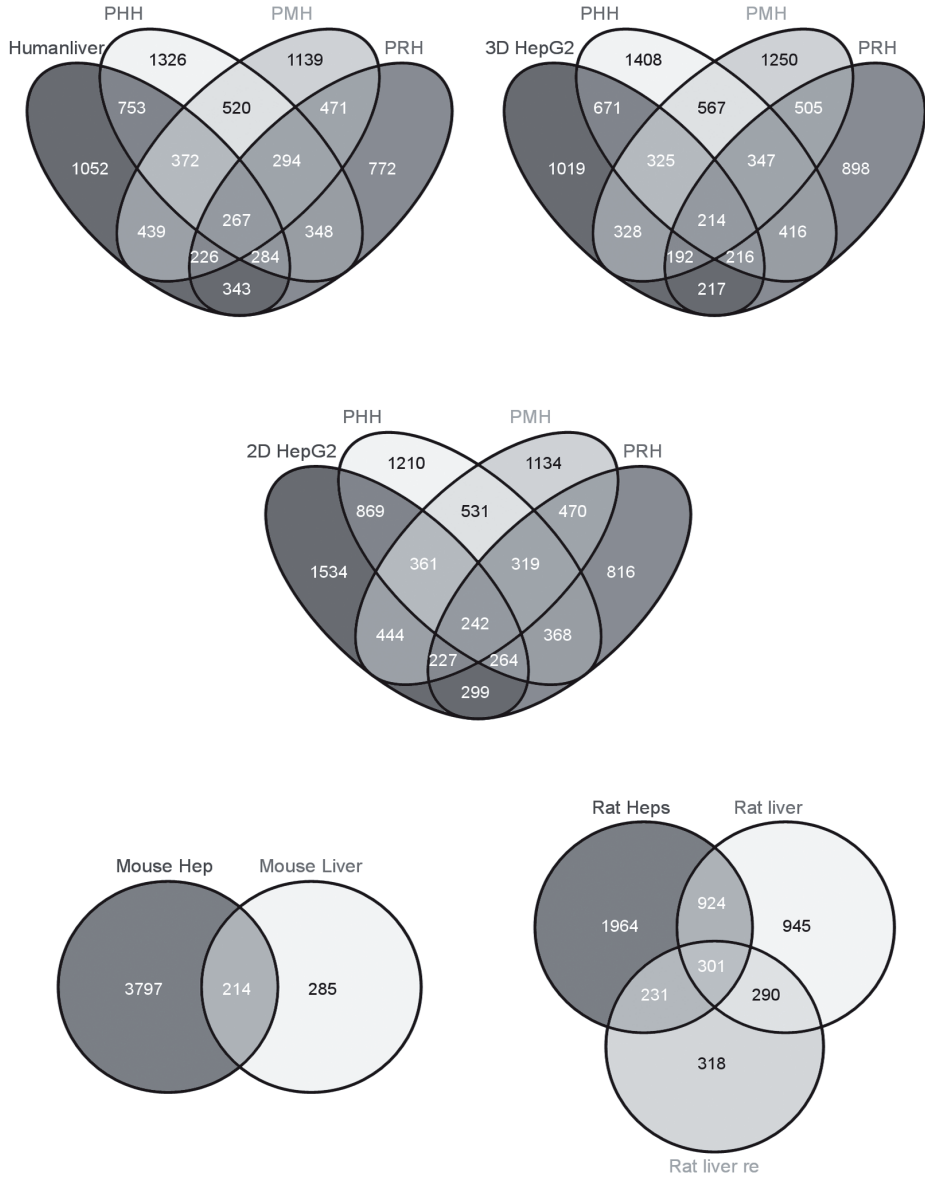
Supplementary S2. Venn diagrams of DEG's upon diclofenac treatment in human, mouse and rat model systems (PHH- primary human hepatocytes; PMH - primary mouse hepatocytes; PRH - primary rat hepatocytes).

Supplementary S3. Venn diagrams of significantly altered canonical pathways from human, mouse and rat DEG's upon diclofenac exposure.

All human, all mouse and all rat models

Supplementary S4. List of pathways that overlap between human *in vitro* models and primary hepatocytes of human, mouse and rat. (PHH- primary human hepatocytes; PMH - primary mouse hepatocytes; PRH - primary rat hepatocytes).

Molecular pathways that are common between 3D HepG2_PHH_PMH_PRH	
Ingenuity Canonical Pathways	**-log(p-value)**
Cell Cycle: G1/S Checkpoint Regulation	4.01E+00
NRF2-mediated Oxidative Stress Response	3.59E+00
Tryptophan Degradation X (Mammalian, via Tryptamine)	3.09E+00
Putrescine Degradation III	3.09E+00
tRNA Charging	2.99E+00
Tyrosine Degradation I	2.87E+00
Dopamine Degradation	2.73E+00
Hepatic Fibrosis / Hepatic Stellate Cell Activation	2.24E+00
Noradrenaline and Adrenaline Degradation	2.20E+00
Complement System	2.20E+00
PXR/RXR Activation	2.18E+00

Mevalonate Pathway I	2.07E+00
Histamine Degradation	2.07E+00
Choline Biosynthesis III	2.00E+00
Phenylalanine Degradation IV (Mammalian, via Side Chain)	1.94E+00
Colanic Acid Building Blocks Biosynthesis	1.94E+00
Asparagine Biosynthesis I	1.93E+00
Fatty Acid α-oxidation	1.88E+00
Oxidative Ethanol Degradation III	1.88E+00
RAN Signaling	1.83E+00
Superpathway of Geranylgeranyldiphosphate Biosynthesis I (via Mevalonate)	1.83E+00
Ethanol Degradation IV	1.77E+00
FXR/RXR Activation	1.76E+00
D-myo-inositol (1,4,5)-trisphosphate Degradation	1.73E+00
Aryl Hydrocarbon Receptor Signaling	1.68E+00
Serotonin Degradation	1.63E+00
Taurine Biosynthesis	1.63E+00
Glycine Biosynthesis I	1.63E+00
Antioxidant Action of Vitamin C	1.60E+00
Phospholipases	1.57E+00
Polyamine Regulation in Colon Cancer	1.56E+00
Tumoricidal Function of Hepatic Natural Killer Cells	1.49E+00
Superpathway of D-myo-inositol (1,4,5)-trisphosphate Metabolism	1.49E+00
Xenobiotic Metabolism Signaling	1.49E+00
Pancreatic Adenocarcinoma Signaling	1.43E+00
Superpathway of Cholesterol Biosynthesis	1.40E+00
Heme Degradation	1.33E+00
Phenylethylamine Degradation I	1.33E+00
Melatonin Degradation II	1.33E+00
Arginine Degradation I (Arginase Pathway)	1.33E+00
NAD Biosynthesis III	1.33E+00
L-cysteine Degradation I	1.33E+00
Ethanol Degradation II	1.31E+00
p38 MAPK Signaling	1.31E+00

Molecular pathways that are common between 2D HepG2_PHH_PMH_PRH	
Ingenuity Canonical Pathways	**-log(p-value)**
4-hydroxyproline Degradation I	3.76E+00
tRNA Charging	2.82E+00
Superpathway of Serine and Glycine Biosynthesis I	2.60E+00
Tumoricidal Function of Hepatic Natural Killer Cells	2.43E+00
Complement System	2.07E+00
NRF2-mediated Oxidative Stress Response	2.04E+00
Cell Cycle: G1/S Checkpoint Regulation	2.02E+00

Hepatic Fibrosis / Hepatic Stellate Cell Activation	2.02E+00
Asparagine Biosynthesis I	1.88E+00
Tryptophan Degradation X (Mammalian, via Tryptamine)	1.74E+00
Putrescine Degradation III	1.74E+00
FXR/RXR Activation	1.60E+00
Lipoate Biosynthesis and Incorporation II	1.58E+00
Proline Degradation	1.58E+00
Taurine Biosynthesis	1.58E+00
Thiosulfate Disproportionation III (Rhodanese)	1.58E+00
Glycerol-3-phosphate Shuttle	1.58E+00
Glycine Biosynthesis I	1.58E+00
Apoptosis Signaling	1.54E+00
VEGF Signaling	1.52E+00
Dopamine Degradation	1.51E+00
Induction of Apoptosis by HIV1	1.37E+00
Aldosterone Signaling in Epithelial Cells	1.31E+00

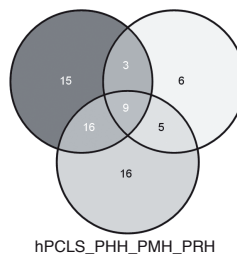| Molecular pathways that are common between human precision cut liver slices_PHH_PMH_PRH	
Ingenuity Canonical Pathways	**-log(p-value)**
Putrescine Degradation III	4.16E+00
Polyamine Regulation in Colon Cancer	3.59E+00
PXR/RXR Activation	3.53E+00
Histamine Degradation	3.22E+00
NRF2-mediated Oxidative Stress Response	2.95E+00
Fatty Acid α-oxidation	2.92E+00
Oxidative Ethanol Degradation III	2.92E+00
Arginine Degradation I (Arginase Pathway)	2.91E+00
Tryptophan Degradation X (Mammalian, via Tryptamine)	2.83E+00
Ethanol Degradation IV	2.75E+00
Cell Cycle: G1/S Checkpoint Regulation	2.66E+00
Acute Phase Response Signaling	2.50E+00
Dopamine Degradation	2.48E+00
Hepatic Fibrosis / Hepatic Stellate Cell Activation	2.41E+00
Sucrose Degradation V (Mammalian)	2.38E+00
Tumoricidal Function of Hepatic Natural Killer Cells	2.31E+00
Retinoate Biosynthesis I	2.08E+00
LXR/RXR Activation	2.07E+00
Ethanol Degradation II	2.04E+00
Noradrenaline and Adrenaline Degradation	1.96E+00
Complement System	1.96E+00
Protein Ubiquitination Pathway	1.92E+00
Guanosine Nucleotides Degradation III	1.90E+00
Aryl Hydrocarbon Receptor Signaling	1.88E+00

Acetyl-CoA Biosynthesis III (from Citrate)	1.84E+00
Asparagine Biosynthesis I	1.84E+00
ILK Signaling	1.78E+00
The Visual Cycle	1.71E+00
Small Cell Lung Cancer Signaling	1.71E+00
p38 MAPK Signaling	1.57E+00
Purine Nucleotides Degradation II (Aerobic)	1.56E+00
D-myo-inositol (1,4,5)-trisphosphate Degradation	1.56E+00
Lipoate Biosynthesis and Incorporation II	1.54E+00
Proline Degradation	1.54E+00
4-hydroxyproline Degradation I	1.54E+00
Atherosclerosis Signaling	1.51E+00
Xenobiotic Metabolism Signaling	1.47E+00
LPS/IL-1 Mediated Inhibition of RXR Function	1.47E+00
FXR/RXR Activation	1.47E+00
Apoptosis Signaling	1.41E+00
Serotonin Degradation	1.40E+00
Gluconeogenesis I	1.40E+00
Methionine Salvage II (Mammalian)	1.37E+00
Phospholipases	1.34E+00
HMGB1 Signaling	1.33E+00
Superpathway of D-myo-inositol (1,4,5)-trisphosphate Metabolism	1.33E+00

Common elements in "2D HepG2" and "Human liver":
4-hydroxyproline Degradation I
Cell Cycle: G1/S Checkpoint Regulation
Lipoate Biosynthesis and Incorporation II
Proline Degradation
Apoptosis Signaling

Common elements in "3D HepG2" and "Human liver":
Noradrenaline and Adrenaline Degradation
PXR/RXR Activation
Histamine Degradation
Fatty Acid α-oxidation
Oxidative Ethanol Degradation III
Ethanol Degradation IV
D-myo-inositol (1,4,5)-trisphosphate Degradation
Aryl Hydrocarbon Receptor Signaling
Serotonin Degradation
Phospholipases
Polyamine Regulation in Colon Cancer
Superpathway of D-myo-inositol (1,4,5)-trisphosphate Metabolism
Xenobiotic Metabolism Signaling
Arginine Degradation I (Arginase Pathway)
Ethanol Degradation II
p38 MAPK Signaling

Common elements in "3D HepG2", "2D HepG2" and "Human PCLS":
NRF2-mediated Oxidative Stress Response
Tryptophan Degradation X (Mammalian, via Tryptamine)
Putrescine Degradation III
Dopamine Degradation
Hepatic Fibrosis / Hepatic Stellate Cell Activation
Complement System
Asparagine Biosynthesis I

FXR/RXR Activation
Tumoricidal Function of Hepatic Natural Killer cells

3D HepG2_PHH_PMH_PRH   2D HepG2_PHH_PMH_PRH

15   3   6

9

16   5

16

hPCLS_PHH_PMH_PRH

Supplementary S5. Genes associated with liver diseases from models systems in which the disease state is positively predicted from ingenuity pathway analysis.

## Liver inflammation

Human liver slices

ABCB4	ABCC2	ADIPOR2	APOB	CAMLG	CCL2
CCL8	CD274	COL3A1	CXCL1		
CXCL10	CXCL2	CYP2E1	DDX5	FKBP1A	GSTP1
IFNAR1	IFNAR2	IL10	RBIL8	INSR	MMP9
MTOR	NAGLU	PEMT	POR	PPARA	PPARG
PPP3CA	PPP3CBP	PP3CC	RASSF1	SOD2	THOP1
TIMP1					

Primary human hepatocytes

ABCB4	ABCC2	ADIPOR2	AGTR1	APOB	CAMLG
CSF1	CXCL1	CXCL10	CXCL2	CYP2E1	EPO
GSTP1	IL8	NR3C1	PDE3B	POLA1	POLB
POLD1	POR	PPARA	PPP3R1	RASSF1	
SLC10A1	SLCO1B1	SOD2	THOP1		

3D HepG2

ADIPOR2	ADK	AGTR1	AMY2B	CAMLG	EPO
IFNGR1	IL8	IMPDH2	NR3C1	PEMT	POLA1
POR	PPARG	PPP3CA	PPP3R1	SLC6A4	TNFRS-
F1A					
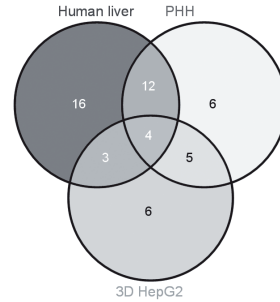
Liver Hyperplasia

Human liver slices

A1BG	ABCC2	ABCC3	ADAM17	ADAM9	ADH1C
AKR1B10	AKR1D1	ALDOB	ANXA2	APOA5	ARPC5
ATF5	ATP1B3	AXIN1	C1S	C7	CA2
CASD1	CASP8	CDC25B	CDK14	CDK5	CD-
KN1B	CHUK	CKS2	CP	CSE1L	CTNNB1
CTSD	CYP1A1	DGAT2	DPP3	DSE	DYNLL1
EIF2AK2	EIF4E	ELMO1	EPHA2	ERBB3	FAIM
FAM83D	FCN3	FOS	FRK	FUCA1	GOLM1
GOT1	GPAA1	H2AFY	HABP2	HGS	HNRNP-
DL	HPD	HSD17B6	HSP90AA1	HSP90AB1	HSPA8
HTATIP2	IFNAR1	IFNAR2	IL8	ING4	ISG15
JUN	KAT5	KDR	KIT	KNG1	KRAS
LBP	MAPRE1	MDM2	MED30	MMP9	MTOR
NFE2L2	NQO1	NUPR1	OSMR	PDGFRB	PDK4
PFN1	PGK1	PHGDH	PLAUR	PNRC1	POLE4
POR	PPARG	PPP1R3C	PRDX1	PRDX3	PTEN
PTGS2	RAD50	RASSF1	RASSF5	RB1	RDH16
RELA	RELB	RIOK1	RNMT	RPL4	RRM1
S100A4	SERPINE1	SLC22A9	SLC35C1	SLC47A1	SL-
CO1B3	SPARC	SRRT	SULF2	TMX2	TOP2B
TPI1	TRIM8	TUBB4B	TXN	TYMS	USP9X
VEGFA	VPS37A	VTN	WBSCR22	YWHAG	

Primary human hepatocytes

A1BG	AADAC	ABCB1	ABCC2	ABCC3	ABCC6
ADAM17	ADH1B	AKR1B10	AKR1C1/AKR1C2		ALDOB
ANXA1	ARID2	ARSE	ASF1B	ATP1B3	AURKA
BAG2	BCL2L1	BSG	C4BPA	C9	CA2
CA9	CAP2	CASD1	CCNB1	CCND1	CD44
CDK5	CDK5RAP3	CDKN1A	CENPH	CKS2	COPG1
CP	CREB3L3	CRELD2	CSF1	CSPP1	CY-
P1A1	DGAT2	DLC1	DSE	DYNLL1	E2F5
ECT2	EIF1AX	ELMO1	ENPP2	EPCAM	EPHA2
ERBB2	ERBB3	FAIM	FAM83D	FGL1	FOXQ1
FUCA1	GC	H2AFY	HABP2	HAMP	HGS
HMGB1	HNRNPDL	HPD	HPX	HSD17B6	HSPA5
HSPA8	IL8	IPO7	ISG15	ITIH4	JUN
KEAP1	LBP	LRG1	MAP3K4	MAT2A	MDM2
MED30	MET	MLF1IP	MT2A	MYO6	NCAPG
NNMT	NPC1	NR1H4	NUPR1	NUSAP1	ORC6
PAQR4	PDK4	PGLYRP2	PHGDH	PKM	PLG
POLD3	POLE	POLE2	POLE3	POLE4	POR
PPP1R3C	PSEN1	RAD50	RASAL2	RASSF1	RB1
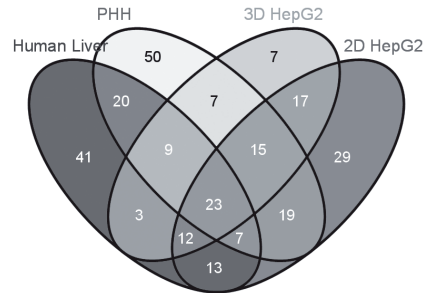
RDH16 RELA RIOK1 RNMT RRM1 RRM2 S100A4 SCP2 SERPINE1 SLC10A1
SLC15A1 SLC22A1 SLCO1B1 SMO SMYD5 SOX4 SQLE SRRT SULF2 TACSTD2
TBP TDO2 TFCP2 TM4SF1 TMX2 TOP2A TPX2 TRIM8 TUBB4B TYMP
TYMS UBE2C UBE2T UCHL1 UGT1A6 VEGFA VTN WHSC1

3D HepG2
ABL1 ADAM17 AKR1D1 ANLN APOA5 ARPC5 ASRGL1 ATAD5 ATP1B3 AURKA
AXIN2 BIRC5 CASD1 CASP2 CASP8 CCDC138 CCNB1 CDC25B CDK5 CDKN3
CKS2 CSE1L CTNNB1 CYP1A1 DGAT2 DKK1 DSE E2F5 ECT2 EIF1AX
ENPP2 EPHA2 ERBB3 FAM83D FOS GLUD1 GOT1 GSTT1 H2AFY HAMP
HEATR6 HGS HPD IGFBP3 IL8 ISG15 JUN MAP3K4 MAVS MDM2
MED30 MLF1IP MT2A NCAPG NPC1 NQO1 NUPR1 NUSAP1 ORC6 OSMR
PGK1 PKM PLK4 POLE2 POLE4 POR PPARG RIOK1 RNMT RPL13A
RRM1 RRM2 S100A4 SCP2 SERF2 SERPINE1 SLC2A1 SOAT2 SOCS1 SQSTM1
SRRT STAT3 SULF2 TM4SF1 TOP2A TP53 TPI1 TPX2 TUBB4B TYMS
UBE2C VEGFA VPS37A

2D HepG2
AADAC ABCB1 ABCC1 ABCC2 ABCC5 ABCC6 ADAM17 AKR1B10 AKR1C1/AKR1C2
AKR1D1 APOA5 ARL2 ASF1B ASRGL1 ATAD5 ATF5 ATP1B3 AXIN2 B4GALT1
BIRC5 BRAF C7 CASP2 CASP8 CCDC138 CCNB1 CDC25B CDK5 CDKN1B
CDKN3 CRELD2 CSE1L CST3 CTNNB1 CTSD DGAT2 DKK1 DLC1 E2F5
E2F8 EIF1AX EIF3H ENPP2 EPHA2 GDPD1 GOT1 GPAA1 GSTT1 HAMP HEATR6
FGFR1 FOS FOXQ1 FRK GDPD1 GOT1 GPAA1 GSTT1 HAMP HEATR6
HMGB1 HP HPD HPX HSPA5 IFT81 IGFBP3 IL8 ING4 ISG15
JUN KCTD2 LETM1 LMCD1 LRG1 MAP3K4 MCRS1 MDM2 MED30 MMP2
MYO6 N4BP2L2 NCAPG NFE2L2 NKD1 NPC1 NRAS NUPR1 ORC6 OSMR
PAQR4 PFN1 PGK1 PIK3CA PIK3IP1 PKM PLK4 PNRC1 POLD3 POLE
POLE2 POLG POR PPARG PPP1R3C PRPF6 RAD50 RASSF1 RIOK1 RNMT
RRM1 RRM2 S100A4 SERPINA6 SERPINC1 SERPINE1 SLC2A1 SLC35C1 SMO SOAT2
SOX4 SPARC SQSTM1 STAT3 TGFB1 TM4SF1 TOP2A TP53 TRIM8 TUBB4B
TYMS UBE2C UBE2T USP9X VEGFA VPS37A

## Liver Steatosis

Human liver slices
ACACA ACOX1 ACOX2 ADIPOR2 APOB AR
CAT CCL2 CYP2E1 FABP4 GNMT GSTP1
NPHP3 PEMT PLIN2 PPARA PPARG PPARG-
C1A SOD2 UCP2

Primary human hepatocytes
ACADL ACOX1 ACOX2 ADIPOR2 APOB CD44
CYP2E1 CYP4A11 GSTP1 HMGCR MOGAT2
MOGAT3 PDE3B PLIN2 PPARA PPARGC1A SOD2
SPP1 SREBF1

2D HepG2
ACOX2 CAT CPT1A DGAT1 FASN
MOGAT3 PDE8A PEMT PLIN2 PPARA PPARG
PPARGC1A TNFRSF1A UCP2
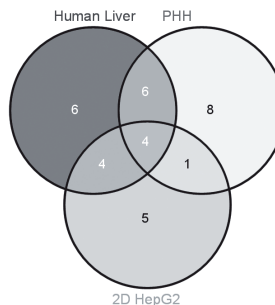
Liver Cholestasis

Human liver slices
ABCB4 ABCB6 ABCB7 ABCC2 ABCC3 ABCG1
ABCG2 ADH1C ADH4 AKR1C3 AKR1D1 BAAT
CAT CYP27A1 CYP7B1 GPX2 IL8 LBP
LIPA MGST2 NR0B2 RDH16 SCD
SLC12A2 SLC25A13 SULT1A2 UGP2 UGT2B15

Primary human hepatocytes
ABCB4 ABCB6 ABCC2 ABCC3 ABCG2 ACSL1
ADH4 ADH6 APOA1 ATP8B1 BAAT CY-
P27A1 HDLBP HMGCR HPX IL8 LBP
LIPC MGST2 MGST3 NR0B2 NR1H4 PAH
RDH16 SCD SCP2 SLC10A1 SLC22A1 SL-
C35B1 SLCO1B1 SREBF1 SULT1A1 SULT1A2 UGP2
UGT2B15

3D HepG2
 ABCG2 ACSL1 ADH6 AKR1D1 BLVRA CYP7A1
GK GPX2 HMGCR HNF1B IL8 LIPA
MGST2 MTTP NR0B2 SCP2 SLC25A6 UGP2